Supplementary Information

Designing and tuning components of random terpolymers toward Ampere-hour-scale organic lithium batteries

Xiaoyin Zhang,[a, b] Ke Chen, [c] Pei Tang,[a, b] Ru Xiao,[a, b] Ruogu Xu,[a, b] Tong Yu,[a] Guangjian Hu,[a, b] Hui-Ming Cheng,[a] Zhenhua Sun*[a, b] and Feng Li*[a, b]

a. *Shenyang National Laboratory for Materials Science, Institute of Metal Research, Chinese Academy of Sciences, Shenyang 110016, China.*

b. *School of Materials Science and Engineering, University of Science and Technology of China, Shenyang 110016, China*

c. *School of Chemical Engineering, The University of New South Wales, Sydney 2052, Australia.*

*Corresponding authors: *E-mail: zhsun@imr.ac.cn, fli@imr.ac.cn*

Methods

Chemical Reagents:

2,5-Dibromo-3,4-ethylenedioxythiophene (97%), $Na_2S·9H_2O$ (99.99% metal basis) and 2, 5-dichloro-1, 4-benzoquinone (DCBQ) (≥98%) were purchased from Aladdin. Sublimed sulfur (≥99.98% metal basis), hexadecyltrimethylammonium bromide (CTAB) (≥99%) and 2, 5-Dichloropyridine (DCPD) (98%) were purchased from Sigma-Aldrich. 1, 2, 3-trichloropropane (TCP) (≥98%) was purchased from Alfa Aesar. N-Methylpyrrolidone (NMP) (≥99.0%) was purchased from China National Pharmaceutical Group Corporation. Electrolytes were purchased from DodoChem Corporation.

Synthesis of TP, BTP-1, BTP-3, BTP-5, PTP, P-TP, P-BTP-1, P-BTP-3, P-BTP-5, and P-PTP:

Na_2S_4 solution was synthesized as a sulfur source. $Na_2S·9H_2O$ (4.8 g) and sublimed sulfur (1.92 g) were added to 16.7 ml deionized water in a 50 ml flake under a N_2 atmosphere. A Na_2S_4 solution was prepared by stirring the solution until no precipitation remained. A series of benzoquinone-tetrasulfide polymers (BTP) were synthesized by interfacial polycondensation. First, 292.5 ml deionized water was degassed by vacuuming. Followed by molar ratio, 26.4 mg of DCBQ (TCP:DCBQ=100:1), 79.2 mg of DCBQ (TCP:DCBQ=100:3) and 132.0 mg of DCBQ (TCP:DCBQ=100:5) were dissolved in 1.59 ml of TCP with small amount of NMP as a cosolvent. 2.19 g of CTAB, 7.5 ml of Na_2S_4 solution and DCBQ/TCP solution were added into degassed water under a N_2 atmosphere with a lasting string over 24 hours at 30 °C. The mixture was collected by centrifugation and subsequently thoroughly washed by a filtration system. Finally, all polymers were dried at 60 °C overnight. The synthesis of tetrasulfide polymers (TP) and pyridine-tetrasulfide polymers (PTP) is similar to the synthesis of BTP. The only difference is that 1.59 ml of TCP and 22.2 mg of DCPD dissolved in 1.59 ml of TCP were used instead of DCBQ/TCP solution for TP and PTP, respectively.

P-TP, P-BTP-1, P-BTP-3, P-BTP-5, and P-PTP were fabricated by a reported method.[1]

Polymers and 2,5-Dibromo-3,4-ethylenedioxythiophene were milled in ethnoal followed by a mass ratio of 49:1. Then, the mixtures were put into a vacuum oven at 50 ^{o}C lasting 24 hours to obtain the final products.

Material Characterizations:

The morphology of the samples was characterized by a scanning electron microscope (Verios G4 UC, 15 kV) equipped with an Oxford EDS analysis system (Ultim Max 100). The cross sections of the Li anode were fabricated and photographed by a focused ion beam (FIB, Helios G4 PFIB CXe DualBeam system of Thermofisher scientific with a Xe ion source), and subsequently, the EDS elemental maps of the lithium anode were characterized by an Oxford EDS analysis system (Ultim Max 100). TEM were obtained by transmission electron microscopy (TEM, Tecnai F20). TGA was performed by a NETZSCH STA 449 C thermos-balance in an Ar atmosphere with 10 °C min^{-1} from room temperature to 600 °C. XPS was performed by an ESCALAB 250 instrument with Al Kα radiation (15 kV, 150 W) under 4×10^{-8} Pa. Raman spectra were collected with a 532 nm or 632.8 nm laser under ambient conditions by JY HR800 instrument. Attenuated total reflectance Fourier transform infrared spectroscopy (ATR-FTIR) was used to characterize the functional groups of the samples by Nicolet iS5 iD7 ATR spectrometer. In the *ex-situ* infrared spectra test, cells at different discharge/charge states are dissembled in a glove box with Ar atmosphere and are directly measured by ATR-FTIR without any purity. A time-of-flight secondary ion mass spectrometer (TOF-SIMS 5, ION-TOF) at a pressure below 10^{-9} Torr was used to analyze the chemical composition of cycled cathodes. The electrical conductivity was measured with ST2742B automatic powder resistency tester from 2 to 20 Mpa.

Electrochemical Measurements:

The polymer cathodes were fabricated by 70 wt% polymer or PEDOT-coated polymer materials, 20 wt% carbon black (Ketjen black EC300J), and 10 wt% poly(vinylidene fluoride) dissolved in NMP as a slurry by a ball-milling method, which was coated onto carbon-coated Al foil and dried under vacuum at 60 °C for over 12 hours. The mass

loading of polymer electrodes (Φ=12 mm) was about 1.2 mg cm^{-2} for the coin cell without the mass loading mentioned. S/KB cathode was synthesized by incorporating 70 wt% sulfur into 30 wt% Ketjen black EC300J by the melting method at 155 °C. The S/KB cathode was fabricated by the same method of the polymer cathode. The electrolytes are 1.0 M LiTFSI and 0.2 M $LiNO_3$ in a solvent mixture of DME and DOL (1:1 v/v). CR2025 type coin cells were assembled in an Ar-filled glovebox with a Celgard 2400 membrane (Φ=19 mm), lithium metal (Φ=15 mm, thickness of 600 μm) as the anode, and 20 μl electrolytes for tests without the polymer/electrolyte ratio mentioned. Galvanostatical Charge-discharge tests were carried out in a voltage range of 1.7-2.8 V (vs Li/Li^+) by a LAND CT2001A instrument. The current density for the tests was calculated based on the mass of polymer or PEDOT-coated polymers (polymers with their PEDOT-coated layers) in the cathode and varied from 100 to 3, 000 mA g^{-1}. Specific capacity of all cells were calculated based on the mass of polymer or PEDOT-coated polymers in the cathode. A VSP-300 multichannel workstation was used to carry out CV tests and EIS measurements.

Pouch-cell Assembly and Evaluation of Energy Density:

First, a mixed slurry (same components with coin cells) was coated onto carbon-coated Al foil. Then, the cathodes (active materials only on one side) were dried under vacuum at 60 °C for over 12 hours. Lithium foil with double lithium metal (100 μm for each single side) is used as the lithium anode. The electrodes were cut intopieces of 4 × 6 cm^2 and 6 × 8 cm^2. Electrodes (4 × 6 cm^2) were used as pouch cells for cycling tests. A 0.7 Ah pouch cells were assembled by 18 pieces of 6 × 8 cm^2 cathodes and 9 pieces of 6 × 8 cm^2 ltihum foil with double lithium metal as anodes. The average polymer areal mass in the cathode is about 1.95 mg cm^{-2}. Celegard 2400 (25 μm) was used as separators. All pouch cells were conducted at 50 mA g^{-1}. The energy density was calculated by the following equation:

$$E = \frac{E_i}{\sum m_i}$$

where E is the gravimetric energy density, E_i is the discharge energy, and m_i is the total

mass of the cathode, anode (200% Li excess is assumed), current collectors (ρ_{Al} ≈2.7 g cm^{-3}, 10 μm and active materials on the two sides are assumed), electrolytes (ρ ≈ 1.1 g cm^{-3}) and separators (ρ ≈ 0.95 g cm^{-3}).

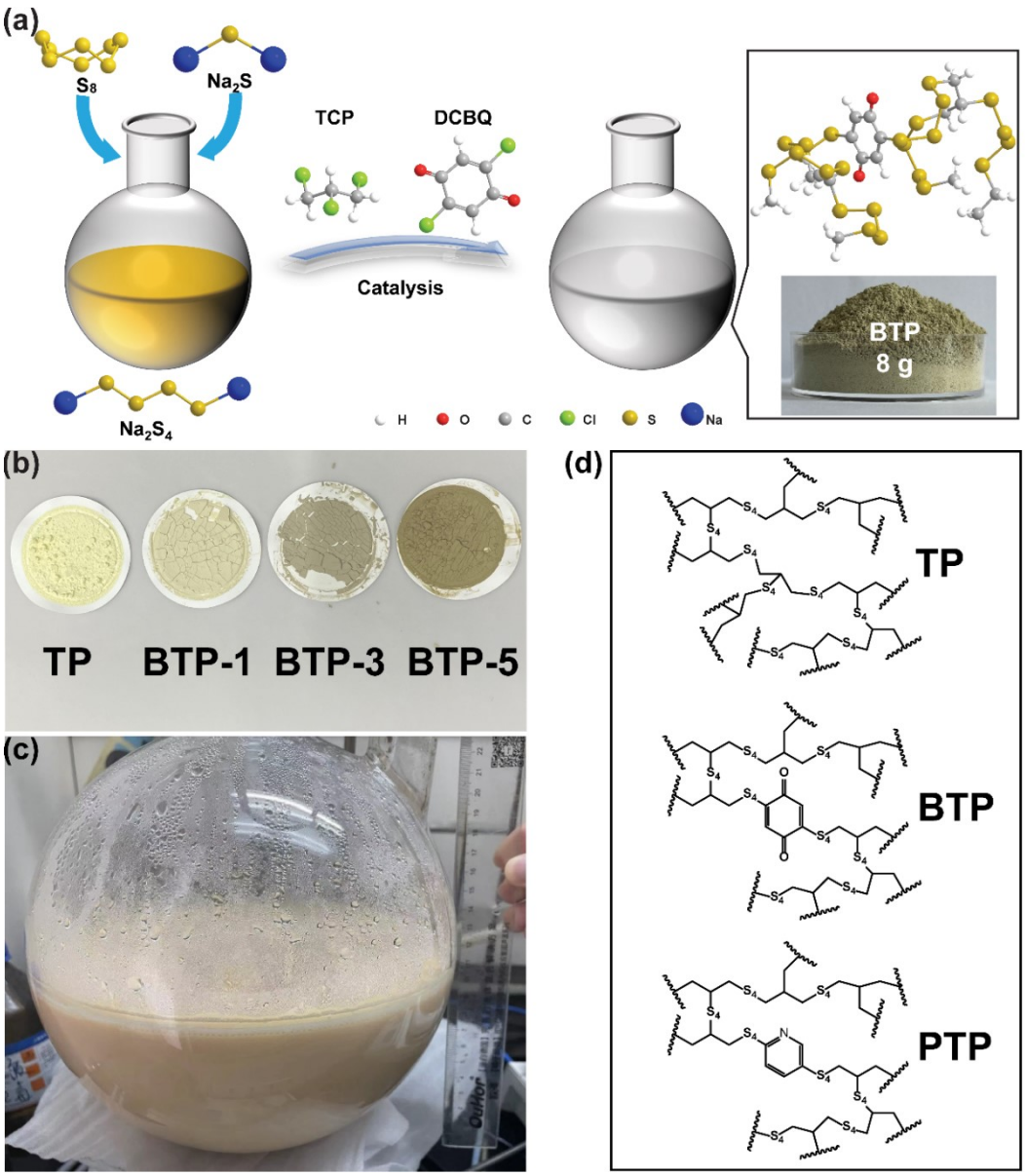

Figure S1. (a) Illustration of the synthesis process of BTPs. The inset image is an optical image of the BTP-1 products during one pot. (b) Optical images of TP, BTP-1, BTP-3 and BTP-5. With increasing amount of benzoquinone groups, the color of polymers changes from faint yellow to light gray, and then dark. (c) Optical image of synthesis process for BTP-1 in a 5L flake at room temperature. (d) Molecular structures of TP, BTP and PTP.

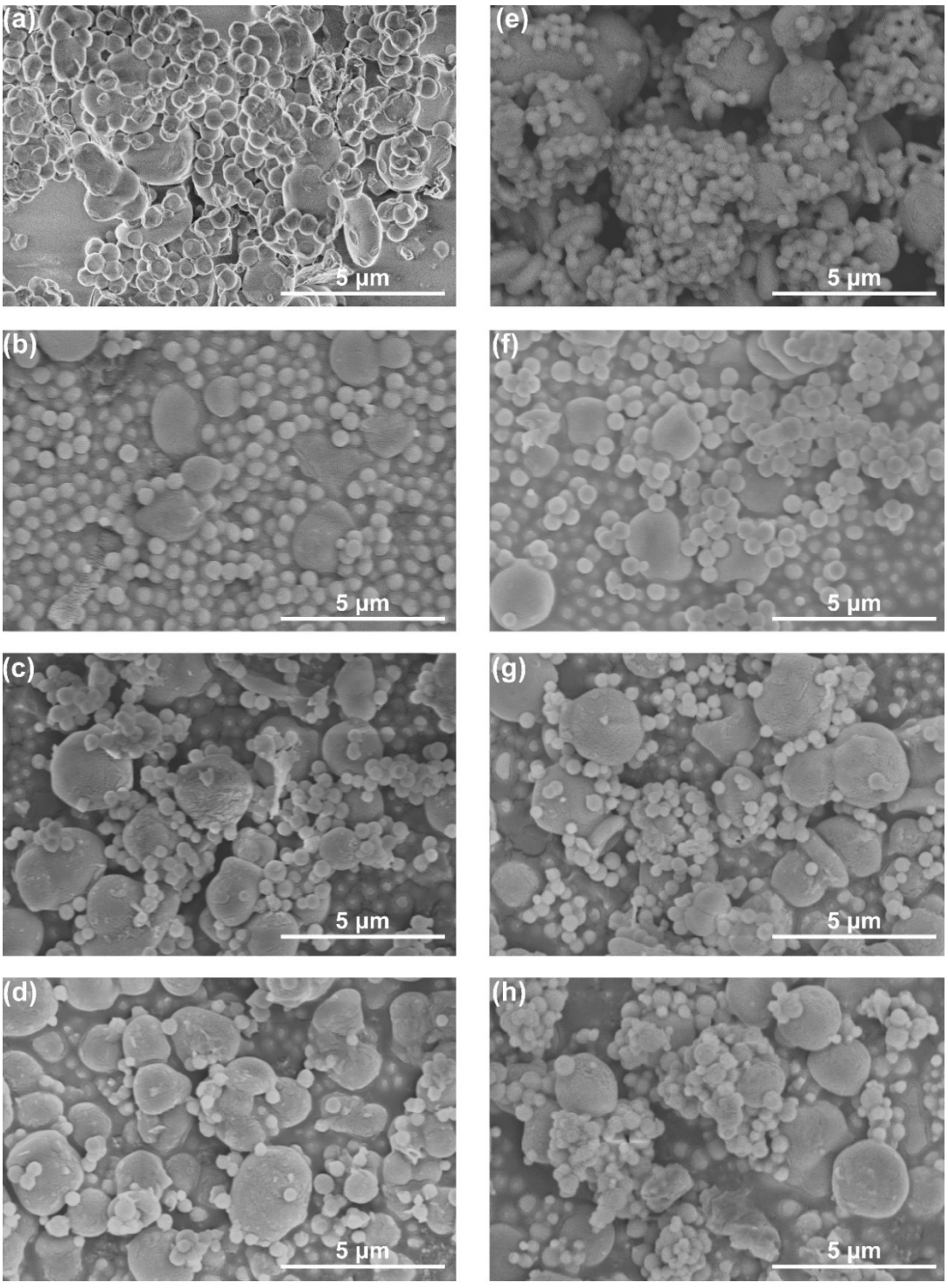

Figure S2. SEM images of (a) TP, (b) BTP-3, (c) BTP-5, (d) P-TP, (e) P-TP, (f) P-BTP-3, (g) P-BTP-5, and (h) P-PTP.

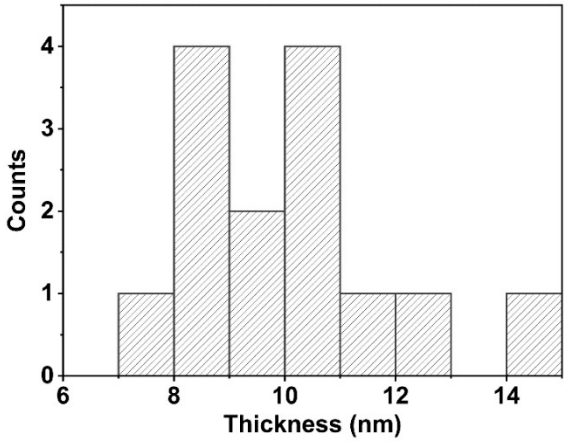

Figure S3. Thickness of PEDOT coated layers based on Figure 1e. Statistical result were collected by randomly measuring thickness of PEDOT layers in Figure 1e.

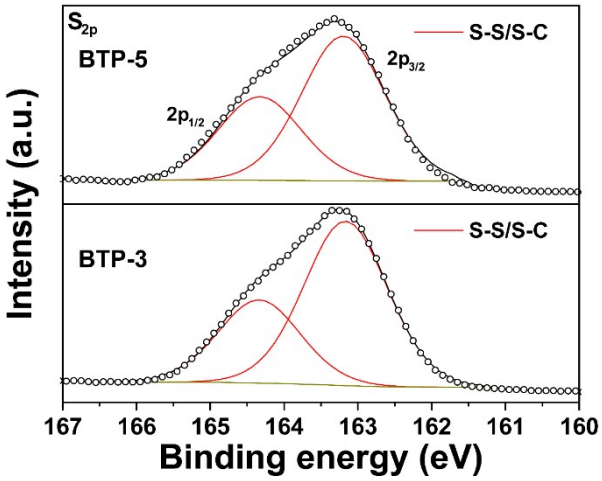

Figure S4. S_{2p} XPS spectra of BTP-3 and BTP-5.

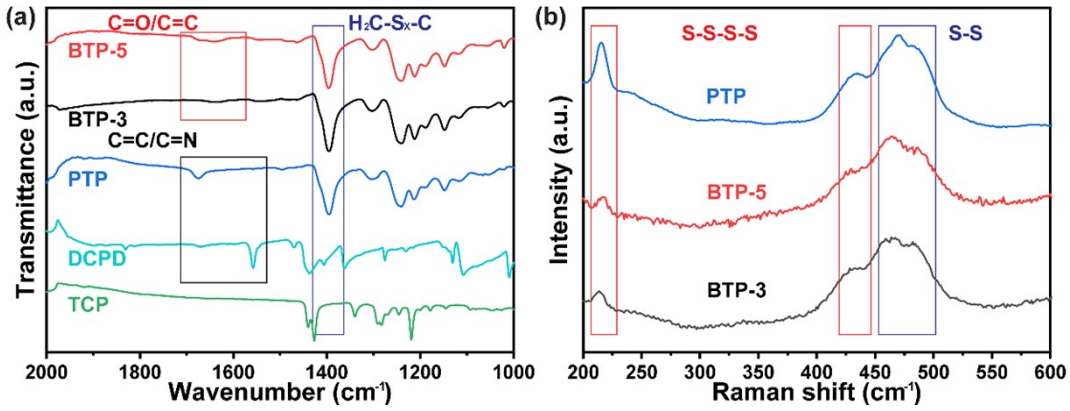

Figure S5. (a) FTIR spectra of BTP-3, BTP-5, TCP, DCPD and PTP. (b) Raman spectra of BTP-3, BTP-5 and PTP.

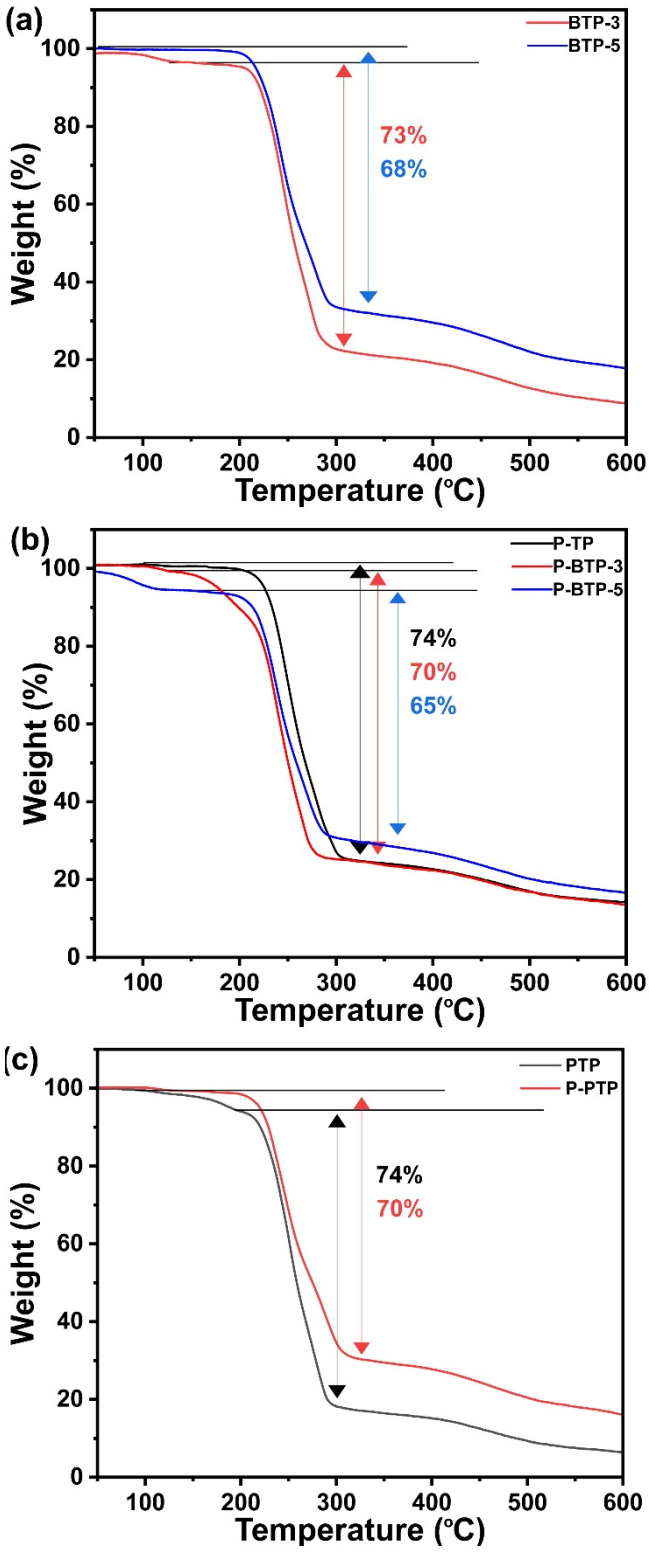

Figure S6. (a) TG curves of BTP-3 and BTP-5. (b) TG curves of P-TP, P-BTP-3 and P-BTP-5. (c) TG curves of PTP and P-PTP.

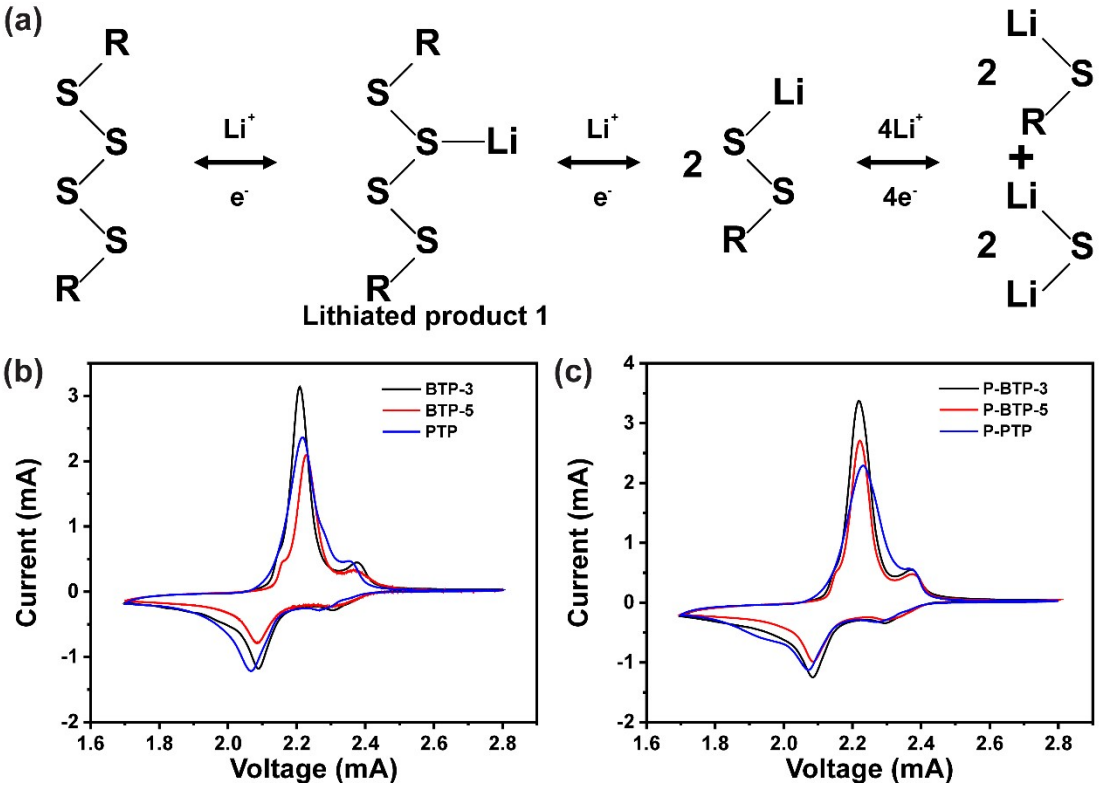

Figure S7. (a) Proposed electrochemical process of polymer cathodes. In the terpolymers, the propyl group as the main R group is electron-donating group. The electron-donating group raises the LUMO energy of the neighboring sulfur atoms corresponding to a lower reduction potential. Thus, lithium ions may prefer to bond to sulfur atoms in the middle of the sulfur chain during the reduction process. (b) CV curves of BTP-3, BTP-5and PTP at 0.1 mV s^{-1}. (c) CV curves of P-BTP-3, P-BTP-5 and P-PTP at 0.1 mV s^{-1}.

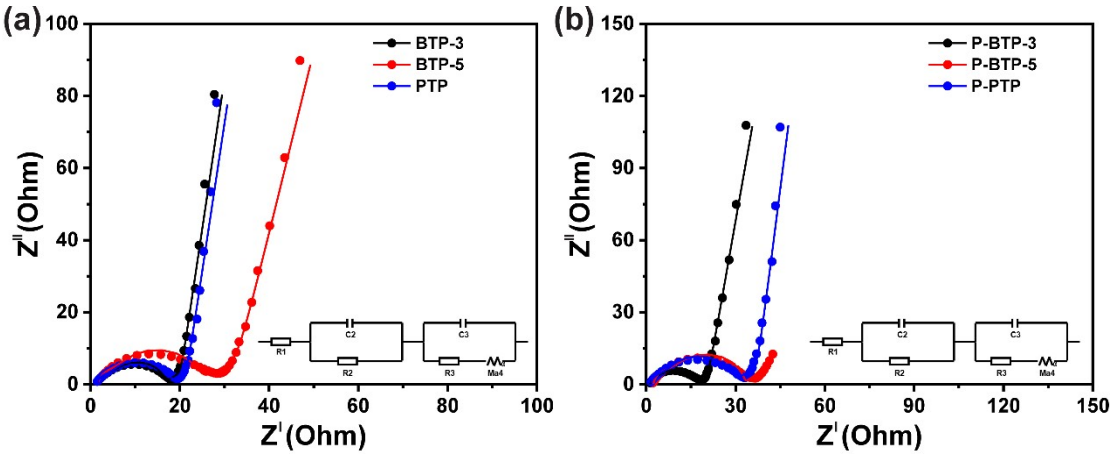

Figure S8. (a) EIS curves of BTP-3, BTP-5 and PTP. (b) EIS curves of P-BTP-3, P-BTP-5 and P-PTP. Insert image is simplified-contact Randles-equivalent circuit.

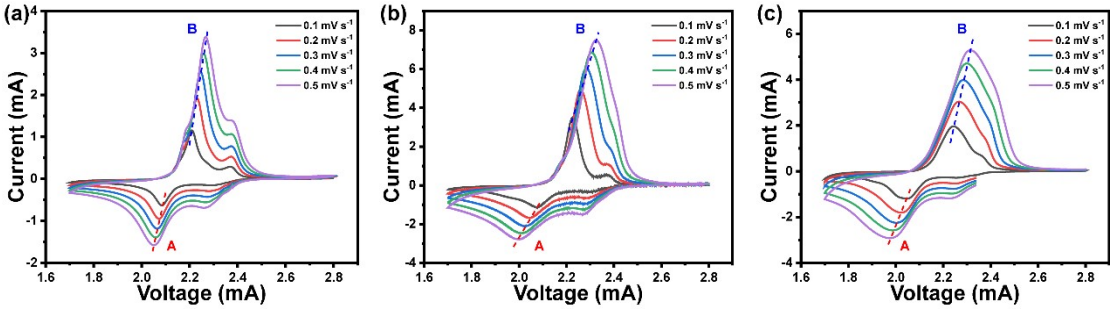

Figure S9. CV curves from 0.1 mV s^{-1} to 0.5 mV s^{-1} of (a) TP, (b) P-BTP-1 and (c) BTP-1 corresponding to fitted lines in Figure 2c and 2d.

The diffusion coefficient of Li ions can be calculated based on the Randles-Sevcik equation:

$$I_p = 2.69 \times 10^5 n^{3/2} A D_{Li}^{1/2} v^{1/2} \Delta c_0$$

Where I_p is the peak current of the cathodic peak at the lower potential, v is the CV scan rate, D_{Li} is the diffusion coefficient of Li ions, n is the number of electron transfer during per redox reaction, A is the area where electrochemical reaction occurs, and Δc_0 is the Li ion concentration within the electrode.

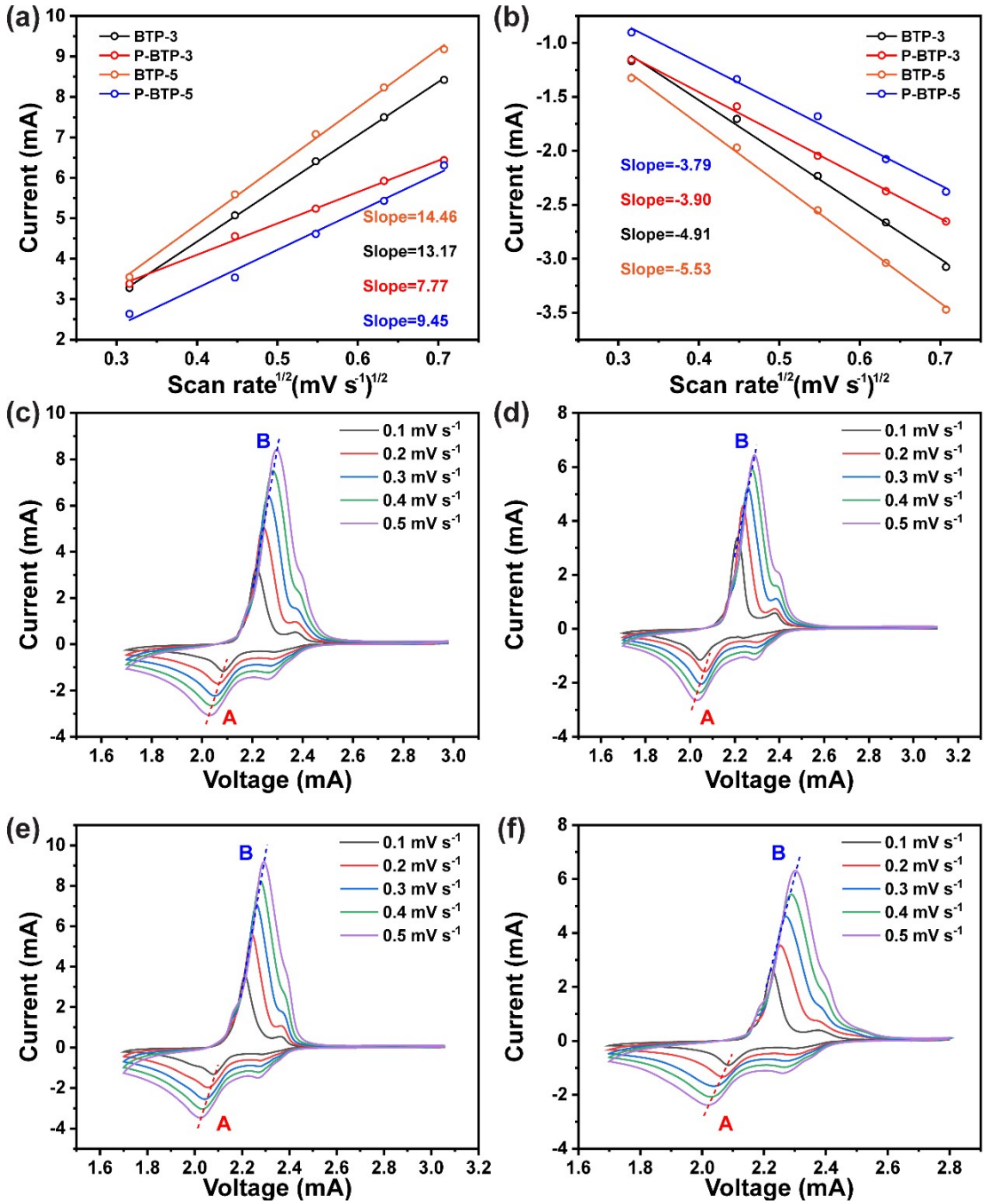

Figure S10. The relationships between peak current I_p at the main peak and square root of scan rate $(mV/s)^{1/2}$ of BTP-3, P-BTP-3, BTP-5and P-BTP-5 based on CV curves recorded at different scan rates at (a) oxidation process (peak B) and (b) reduction process (peak A). CV curves from 0.1 mV s^{-1} to 0.5 mV s^{-1} of (c) BTP-3, (d) P-BTP-3, (e) BTP-5 and (f) P-BTP-5 corresponding to fitted lines in Figures S10a and S10d.

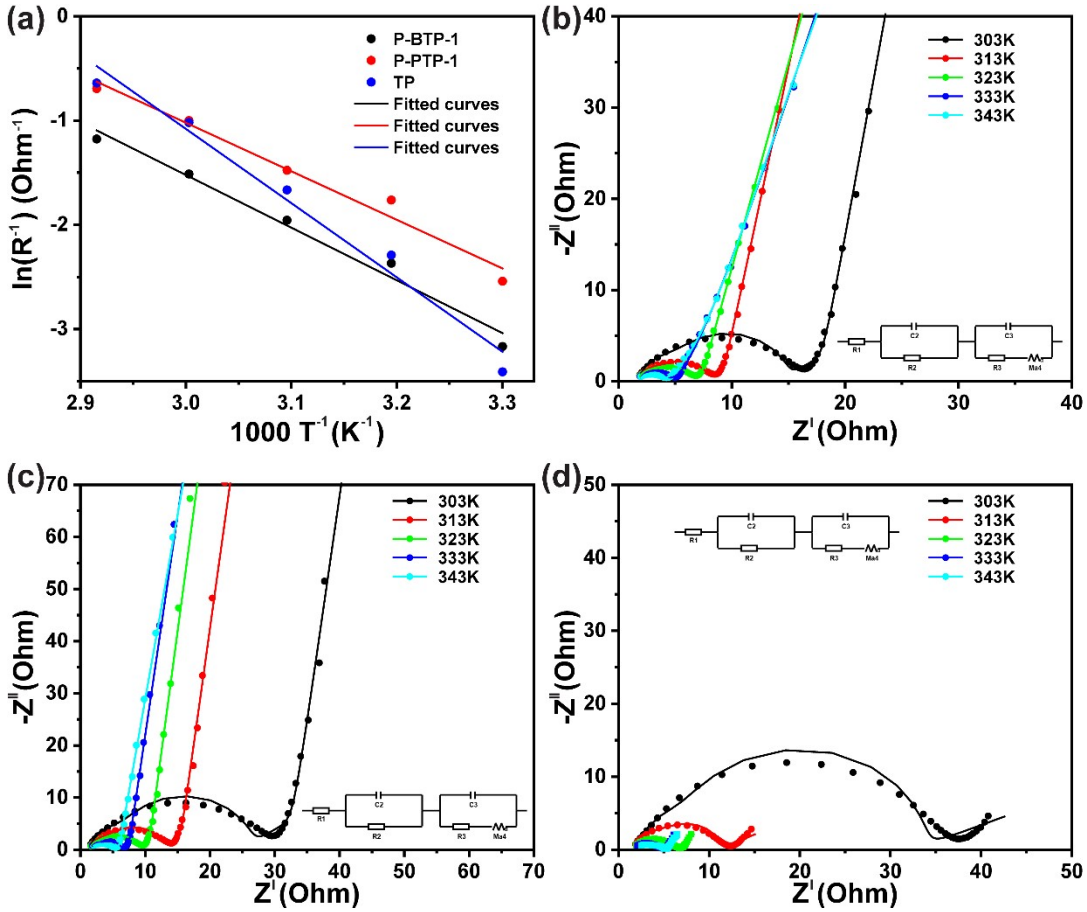

Figure S11. (a) The linear relationship between logarithmic values of the reciprocal of charge transfer resistance and the reciprocal of absolute temperatures of P-BTP-1, P-PTP and TP. EIS curves of (b) P-BTP-1, (c) P-PTP, and (d) TP from 303K to 343K corresponding to fitted lines in Figure S11a.

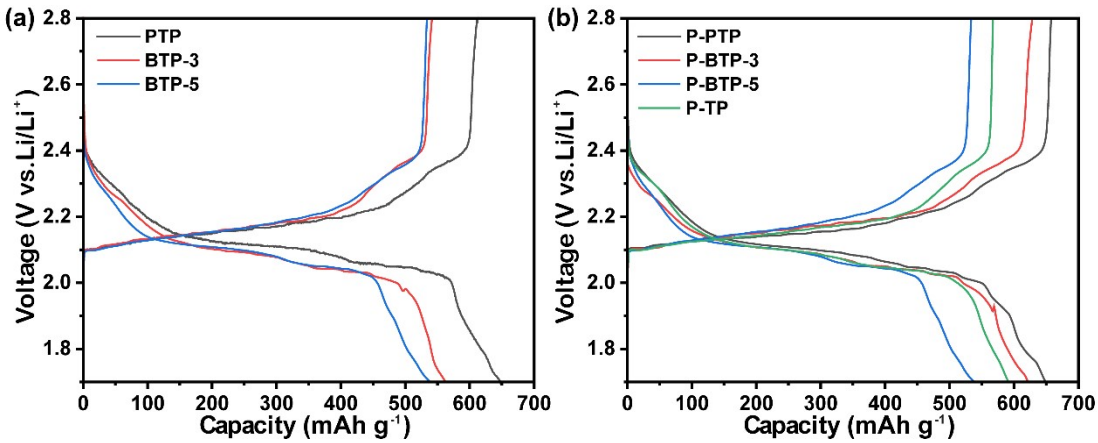

Figure S12. (a) Discharge/charge curves of PTP, BTP-3, and BTP-5 coin cells at 100 mA g^{-1}. (b) Discharge/charge curves of P-TP, P-PTP, P-BTP-3, and P-BTP-5 coin cells at 100 mA g^{-1}. Specific capacity is calculated based on the mass of the polymers or PEDOT-coated polymers.

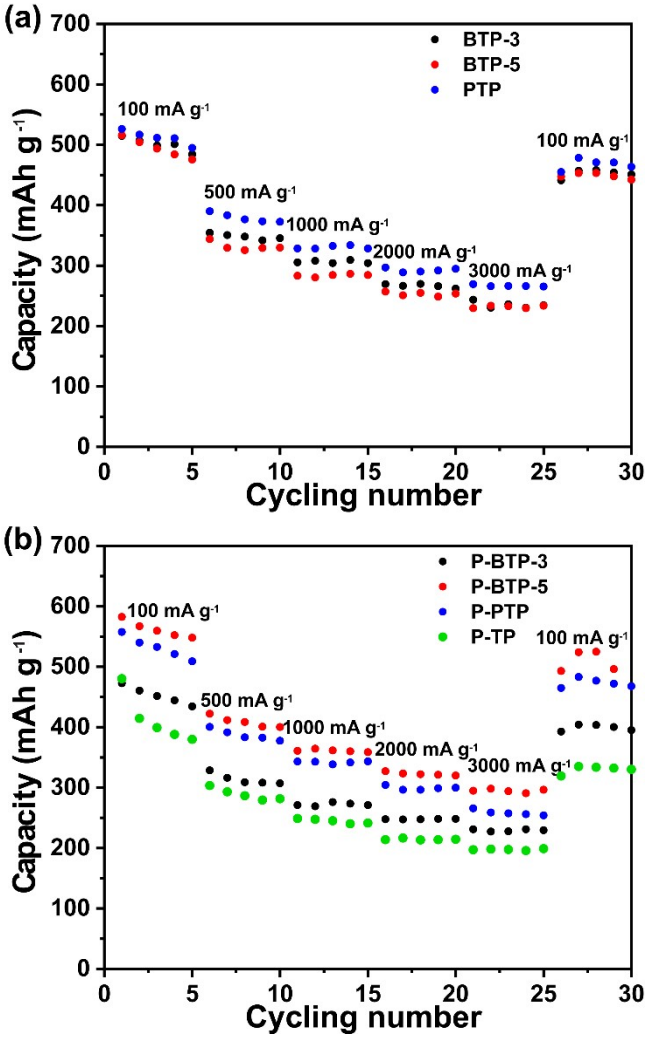

Figure S13. (a) Rate performance of PTP, BTP-3, and BTP-5 coin cells. (b) Rate performance of P-TP, P-PTP, P-BTP-3, and P-BTP-5 coin cells. Specific capacity is calculated based on the mass of the polymers or PEDOT-coated polymers.

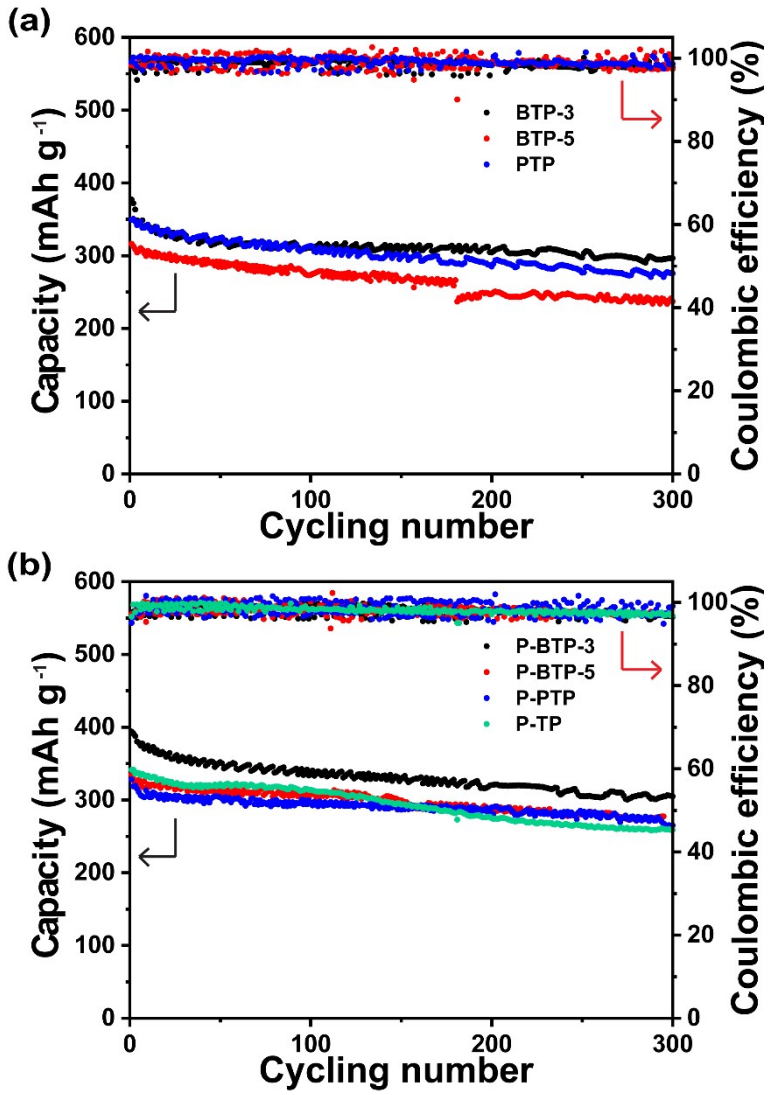

Figure S14. (a) Cycling performance of PTP, BTP-3and BTP-5 coin cells at 1, 000 mA g^{-1}. (b) Cycling performance of P-TP, P-PTP, P-BTP-3, and P-BTP-5 coin cells at 1, 000 mA g^{-1}. Specific capacity is calculated based on the mass of the polymers or PEDOT-coated polymers.

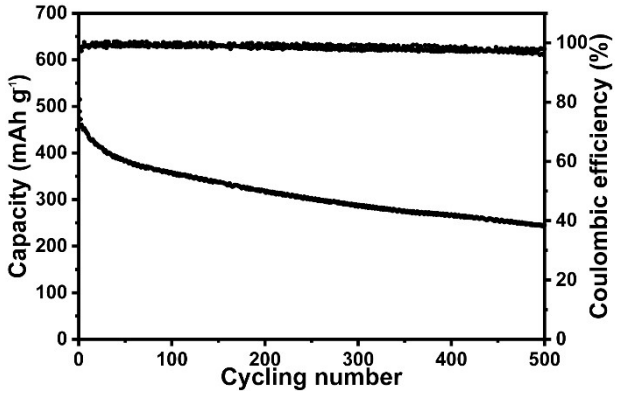

Figure S15. Cycling performance of S/KB coin cell at 1, 000 mA g^{-1}. Specific capacity of S/KB is based on the mass of S/KB hybrids.

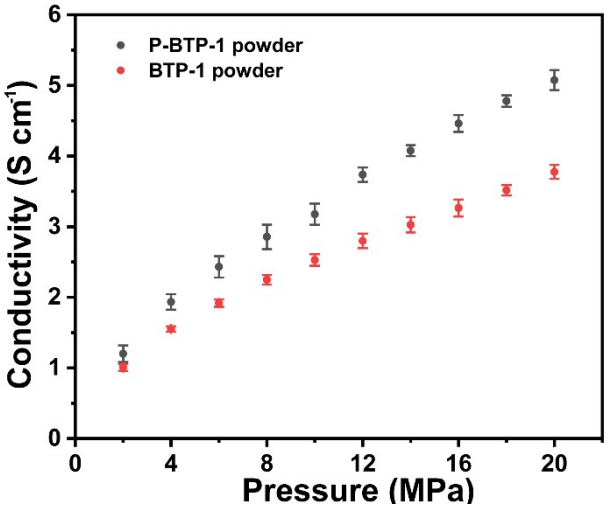

Figure S16. Electronic conductivity of P-BTP-1 powder and BTP-1 powder from 2 to 20 MPa. P-BTP-1 powder or BTP-1 powder were fabricated by ball-milling 70 wt% P-BTP-1 or BTP-1, 20 wt% carbon black (Ketjen black EC300J), and 10 wt% poly(vinylidene fluoride).

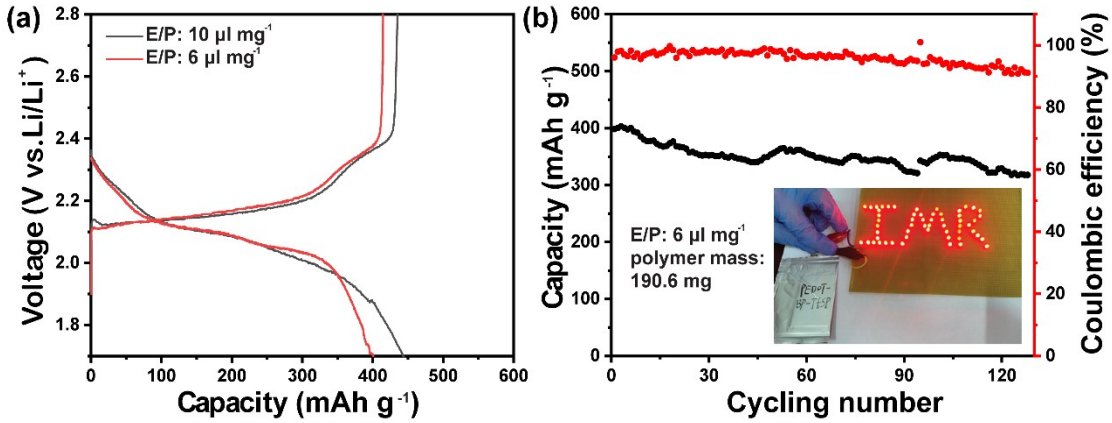

Figure S17. (a) Discharge/charge curves of P-BTP-1 pouch cells at different E/P ratios at 50 mA g^{-1}. (b) Cycling performance of a four-layer pouch cell with P-BTP-1 cathodes at 50 mA g^{-1}. Specific capacity is calculated based on the mass of the polymers or PEDOT-coated polymers.

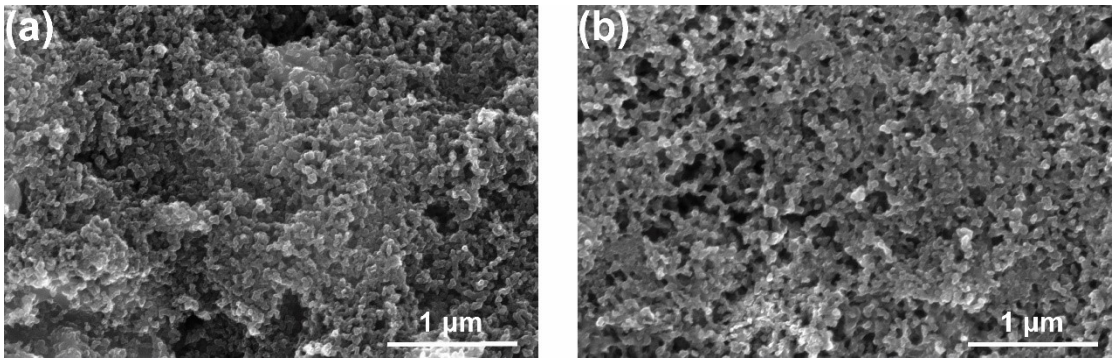

Figure S18. SEM images of P-BTP-1 cathodes (a) at pristine state and (b) after 100 cycles at 1000 mA g^{-1}.

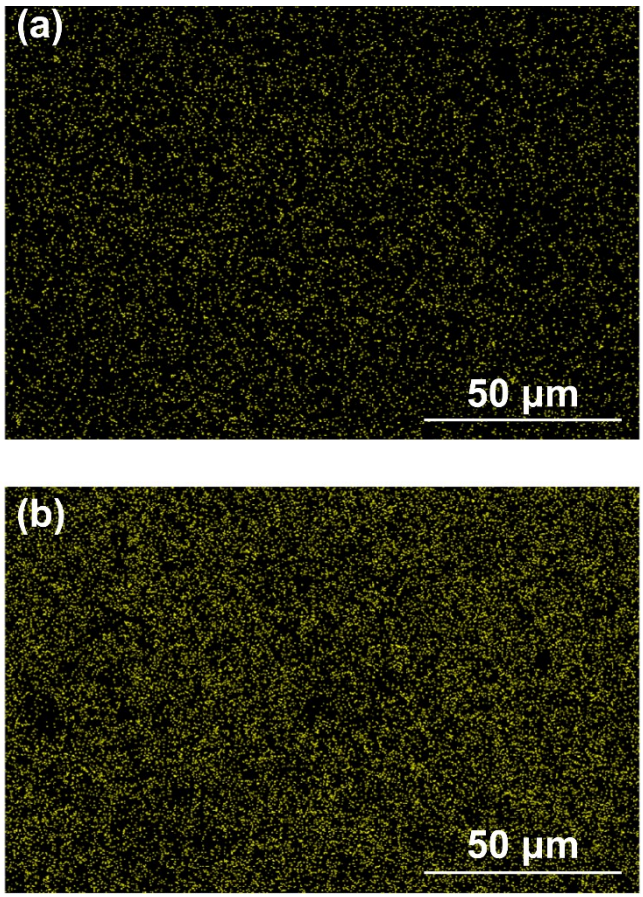

Figure S19. EDS mapping images of top view of lithium metal anode after 100 cycles at 2, 000 mA g^{-1} in (a) P-BTP-1 cells and (b) S/KB cells corresponding to Figure 5a and 5c. Yellow indicates sulfur.

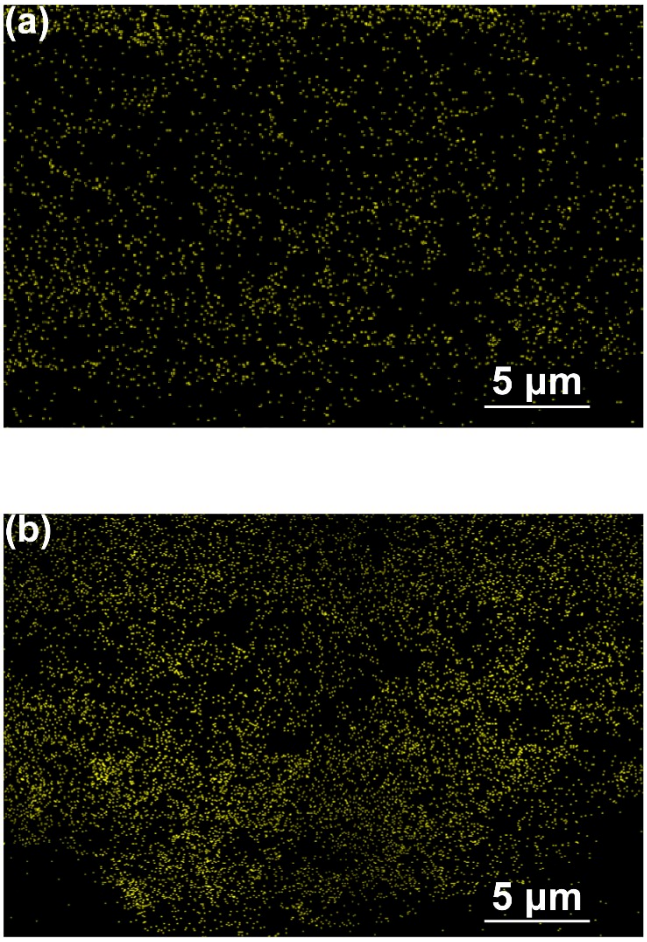

Figure S20. EDS mapping images of cross section of lithium metal anode after 100 cycles at 2, 000 mA g^{-1} in (a) P-BTP-1 cells and (b) S/KB cells corresponding to Figure 5b and 5d. Yellow indicates sulfur.

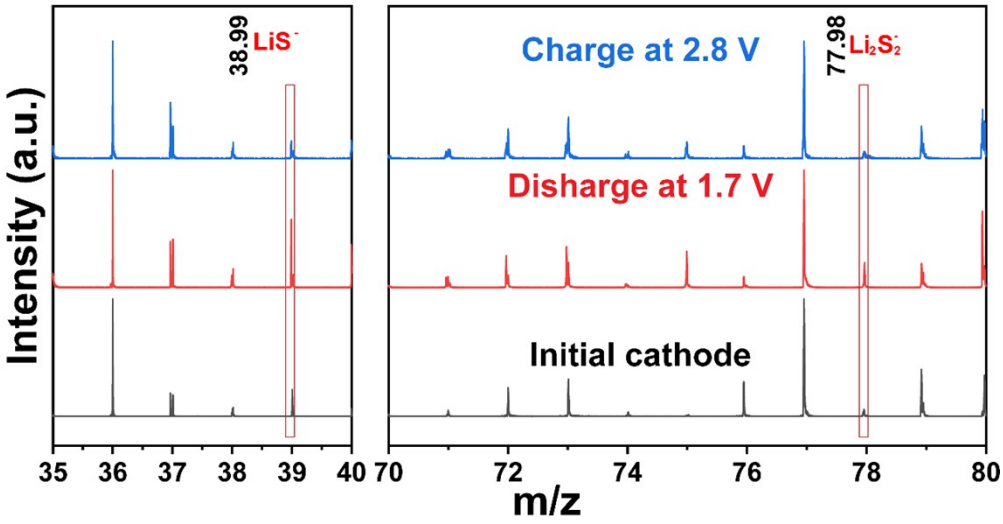

Figure S21. ToF-SIMS results of P-BTP-1 cells at initial cathode, discharge state at 1.7 V and charge state at 2.8V.

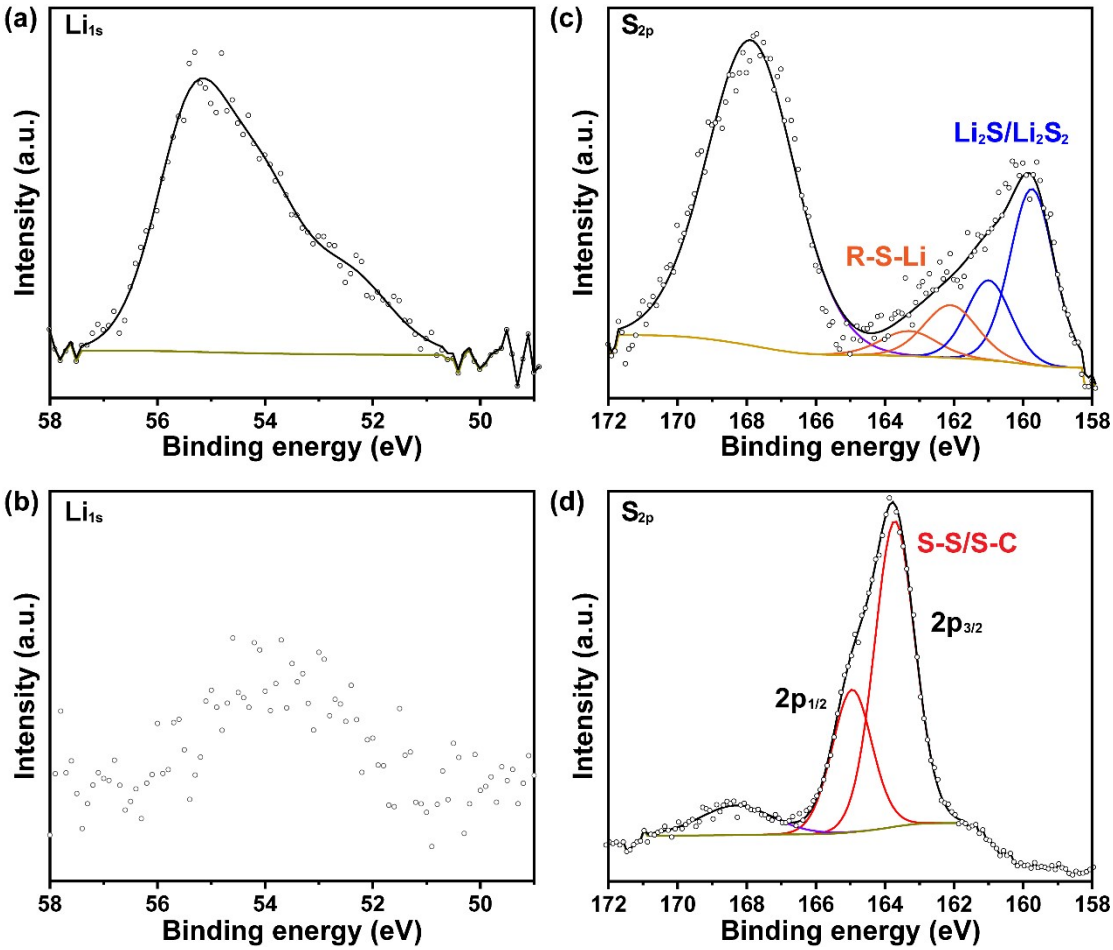

Figure S22. XPS Li_{1s} spectra of (a) P-BTP-1 discharged to 1.7 V and (b) P-BTP-1 charged to 2.8 V. XPS S_{2p} spectra of (c) P-BTP-1 discharged to 1.7 V and (d) P-BTP-1 charged to 2.8 V.

Table S1. Reaction temperature for synthesizing organosulfur polymer cathode materials.

Reaction	Temperature
Inverse vulcanization[2]	Over 180 °C
Sulfurized reaction for SPAN[3]	Over 300 °C
Coupling reaction for OPNS[4]	260 °C
Condensation reaction of thiol monomers*[5, 6]	Room temperature - 40 °C

*H_2S lastingly produce during condensation reaction of thiol monomers.

Table S2. Price of main raw materials for synthesizing terpolymers, BTP-1 and cathode materials of commercial lithium-ion batteries.

Regents	Price (Yuan ton^{-1})
$Na_2S{\cdot}9H_2O$	6500
TCP	8500
Sublime sulfur	3800
BTP-1	~17600
$LiFeO_4$	~155000
NCM532	~350000
$LiCoO_2$	~550000
$LiMnO_2$	~125000

Price of all chemicals is the price at May, 2022.

Price of BTP-1 is roughly estimated by the following equation:

$$P = \frac{\left(0.38P_{Na_sS\cdot 9H_2O} + 0.47P_{TCP} + 0.15P_S\right)}{Y}$$

Where P denotes the price of P-BTP-1 per ton, $P_{Na_sS\cdot 9H_2O}$ denotes the price of $Na_2S{\cdot}9H_2O$ per ton, P_{TCP} denotes the price of TCP per ton, P_S denotes the price of sublime sulfur per ton and Y denotes yield of BTP-1. In this equation, only prices of raw materials are considered. Yield of BTP-1 is about 40% based on fabrication process in 300 ml aqueous solution.

Table S3. Band energy of TP, BTP-1, P-BTP-1, BTP-3, BTP-5 and PTP in XPS S_{2p} spectra.

Polymers	Binding energy of S $2p_{3/2}$ (eV)	Binding energy of S $2p_{1/2}$ (eV)
TP	163.19	164.35
BTP-1	163.14	164.29
P-BTP-1	163.15	164.29
BTP-3	163.16	164.32
BTP-5	163.18	164.32
PTP	163.43	164.57

Table S4. The O content of TP, BTP-1, BTP-3, BTP-5 and PTP by elemental analysis.

Polymers	O content (wt%)
TP	0.038
BTP-1	0.142
BTP-3	0.186
BTP-5	0.343
PTP	0.040

Table S5. Electrochemical performance of organic lithium pouch cells.

Cathode	Capacity (Ah)	Cycling performance	Energy density (Wh kg^{-1})
Lumichrome*[7]	0.08	40 cycles (~33 mAh g^{-1})	Null
DIXPS*[8]	~0.085	50 cycles (~300 mAh g^{-1})	~840
PTS@MSGC*[9]	~0.03	100 cycles (256 mAh g^{-1})	~660
P-TS*[10]	0.05	50 cycles (137 mAh g^{-1})	~320
Poly-BQ1**[11]	Null	1 cycle (~280 mAh g^{-1})	Null
PAQ**[12]	Null	8 cycles (219 mAh g^{-1})	Null
poly(Li_2S_6-r-DIB)**[13]	Null	100 cycles (320 mAh g^{-1})	Null
$Se_{0.05}S_{0.95}$PAN**[14]	0.3	90 cycles (~283 mAh g^{-1})	~763
SPAN**[15]	~0.14	90 cycles (~436 mAh g^{-1})	~1098
P-BTP-1 (this work)	~0.077	130 cycles (321 mAh g^{-1})	850
P-BTP-1 (this work)	~0.7	80 cycles (348 mAh g^{-1})	870

Specific capacity and energy density are based on organic materials.

*The cathodes are organic molecules.

**The cathodes are organic polymers.

References

1. H. Meng, D. F. Perepichka, M. Bendikov, F. Wudl, G. Z. Pan, W. Yu, W. Dong and S. Brown, *J. Am. Chem. Soc.*, 2003, **125**, 15151-15162.
2. W. J. Chung, J. J. Griebel, E. T. Kim, H. Yoon, A. G. Simmonds, H. J. Ji, P. T. Dirlam, R. S. Glass, J. J. Wie, N. A. Nguyen, B. W. Guralnick, J. Park, A. Somogyi, P. Theato, M. E. Mackay, Y. E. Sung, K. Char and J. Pyun, *Nat. Chem.*, 2013, **5**,

518-524.

3. Z. Xu, J. Yang, J. Qian, T. Zhang, Y. Nuli, R. Chen and J. L. Wang, *Energy Storage Mater.*, 2019, **20**, 388-394.
4. H. Hu, B. Zhao, H. Cheng, S. Dai, N. Kane, Y. Yu and M. Liu, *Nano Energy*, 2019, **57**, 635-643.
5. A. Bhargav, M. E. Bell, Y. Cui and Y. Z. Fu, *ACS Appl. Mater. Interfaces*, 2018, **1**, 5859-5864.
6. A. Bhargav, M. E. Bell, J. Karty, Y. Cui and Y. Z. Fu, *ACS Appl. Mater. Interfaces*, 2018, **10**, 21084-21090.
7. J.-S. Yeo, E.-J. Yoo, S.-H. Ha, D.-I. Cheong and S.-B. Cho, *J. Power Sources*, 2016, **313**, 91-95.
8. A. Bhargav and A. Manthiram, *Adv. Energy Mater.*, 2020, **10**, 2001658.
9. X. Lv, W. Guo, J. Song and Y. Z. Fu, *Small*, 2021, **18**, 2105071.
10. M. Mao, S. Wang, Z. Lin, T. Liu, Y. S. Hu, H. Li, X. Huang, L. Chen and L. M. Suo, *Adv. Mater.*, 2021, **33**, 2005781.
11. Y. Zhao, M. Wu, H. Chen, J. Zhu, J. Liu, Z. Ye, Y. Zhang, H. Zhang, Y. Ma, C. Li and Y. Chen, *Nano Energy*, 2021, **86**, 106055.
12. J. Bitenc, A. Vizintin, J. Grdadolnik and R. Dominko, *Energy Storage Mater.*, 2019, **21**, 347-353.
13. F. Dong, C. Peng, H. Xu, Y. Zheng, H. Yao, J. Yang and S. Zheng, *ACS Nano*, 2021, **15**, 20287-20299.
14. Z. Jiang, H. J. Guo, Z. Zeng, Z. Han, W. Hu, R. Wen and J. Xie, *ACS Nano*, 2020, **14**, 13784-13793.
15. Z. Shen, W. Zhang, S. Mao, S. Li, X. Wang and Y. Lu, *ACS Energy Lett.*, 2021, **6**, 2673-2681.